

Role of Histone H3 Lysine 27 Methylation in X Inactivation

Kathrin Plath,^{1*} Jia Fang,^{2*} Susanna K. Mlynarczyk-Evans,¹
 Ru Cao,² Kathleen A. Worringer,¹ Hengbin Wang,²
 Cecile C. de la Cruz,¹ Arie P. Otte,³ Barbara Panning,^{1†}
 Yi Zhang^{2†}

The Polycomb group (PcG) protein Eed is implicated in regulation of imprinted X-chromosome inactivation in extraembryonic cells but not of random X inactivation in embryonic cells. The *Drosophila* homolog of the Eed-Ezh2 PcG protein complex achieves gene silencing through methylation of histone H3 on lysine 27 (H3-K27), which suggests a role for H3-K27 methylation in imprinted X inactivation. Here we demonstrate that transient recruitment of the Eed-Ezh2 complex to the inactive X chromosome (Xi) occurs during initiation of X inactivation in both extraembryonic and embryonic cells and is accompanied by H3-K27 methylation. Recruitment of the complex and methylation on the Xi depend on *Xist* RNA but are independent of its silencing function. Together, our results suggest a role for Eed-Ezh2-mediated H3-K27 methylation during initiation of both imprinted and random X inactivation and demonstrate that H3-K27 methylation is not sufficient for silencing of the Xi.

Dosage compensation in mammals is achieved by transcriptional silencing of one X chromosome in female cells (1). X inactivation is a multistep process involving choice of the active X chromosome, initiation of silencing on the Xi, and maintenance of the

Xi throughout all subsequent cell divisions (2). *Xist* plays a role in each stage of X-chromosome inactivation (3). *Xist* is transcribed exclusively from the Xi in female somatic cells, where *Xist* RNA remains in the nucleus and coats the Xi. The onset of X inactivation correlates with the initial cis-spread of *Xist* RNA to coat the chromosome. The Xi is characterized by a series of epigenetic chromatin modifications including histone H3 methylation, histone H4 hypoacetylation, enrichment of variant histone macroH2A, and DNA methylation (4). Histone methylation plays an important role in regulating gene expression (5–7). The EED-EZH2 PcG complex and its *Drosophila* counterpart, the ESC-E(Z) complex, methylate H3 at Lys²⁷ (H3-K27) (8–11). In *Drosophila*, ESC-E(Z)-me-

diated H3-K27 methylation is required for *HOX* gene silencing (11). Mice homozygous for an *eed* mutation are defective in the maintenance of X-chromosome silencing in extraembryonic, but not embryonic, tissues (12). Eed and Ezh2 are enriched on the Xi in trophoblast stem (TS) cells (13), an extraembryonic cell type, which suggests a role for Eed-Ezh2-mediated H3-K27 methylation in regulation of imprinted X inactivation.

To determine whether H3-K27 methylation accompanies the enrichment of the Eed-Ezh2 complex on the Xi in TS cells, we stained these cells with antibodies that recognize Ezh2 (also referred to as Enx-1) to mark the Xi (13), in combination with antibodies directed against H3-dimethyl-K27 (H3-2mK27) or H3-trimethyl-K27 (H3-3mK27). We observed accumulation of H3-3mK27, but not of H3-2mK27, on the Xi as one large focus that colocalized with the region of Ezh2 accumulation (Fig. 1, fig. S1). It was important to show that the observed Xi enrichment of H3-3mK27 is not due to cross-reactivity of the antibody with H3-trimethyl-K9 (H3-3mK9), because the amino acids in H3 adjacent to K27 are very similar to those surrounding K9. To this end, ELISA (enzyme-linked immunosorbent assay) analysis, peptide competition, and additional immunostainings with an antibody directed against H3-3mK9 showed that there is indeed an enrichment of H3-3mK27, but not H3-3mK9, on the Xi in TS cells (Fig. 1, fig. S2). Together, these data suggest that the Eed-Ezh2 complex mediates the enrichment of H3-3mK27 on the Xi in TS cells. Consistent with these results, histones isolated from *Drosophila* E(Z) mutant embryos and *eed* mutant embryonic stem (ES) cells show a dramatic reduction in levels of H3-3mK27 (14).

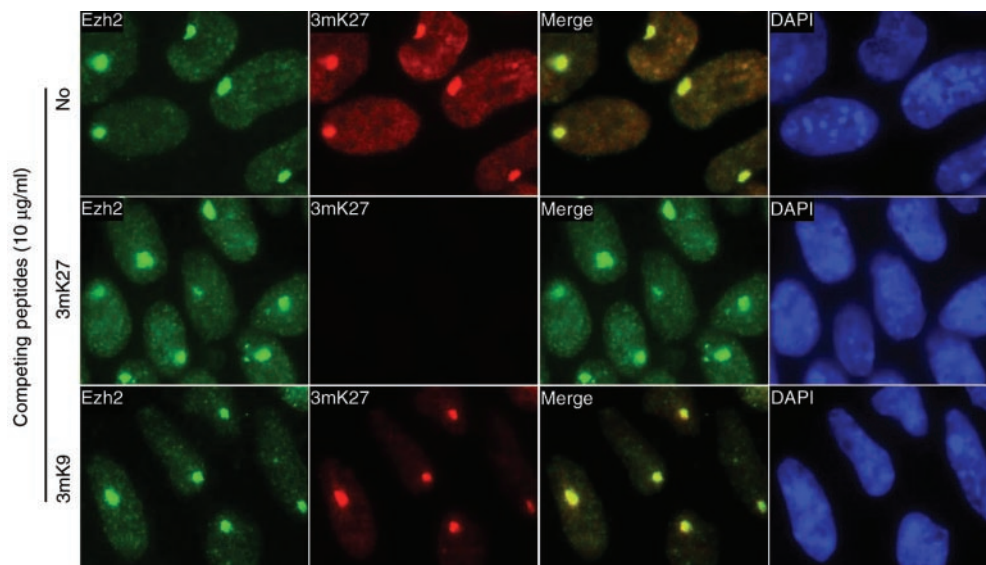
Because Eed is required for maintenance of imprinted X inactivation in differentiated cells of the trophoblast lineage

¹Department of Biochemistry and Biophysics, University of California San Francisco, San Francisco, CA 94143, USA. ²Department of Biochemistry and Biophysics, Lineberger Comprehensive Cancer Center, University of North Carolina at Chapel Hill, Chapel Hill, NC 27599–7295, USA. ³Swammerdam Institute for Life Sciences, BioCentrum Amsterdam, University of Amsterdam, 1018 TV Amsterdam, Netherlands.

*These authors contributed equally to this work.

†To whom correspondence should be addressed. E-mail: yi_zhang@med.unc.edu; bpanning@biochem.ucsf.edu

Fig. 1. Colocalization of Eed and H3-3mK27 on the Xi in extraembryonic cells. TS cells were stained with Ezh2 and H3-3mK27 antibodies as indicated. The merged image consists of Ezh2 (green) and H3-3mK27 (red), and nuclei are stained with 4',6'-diamidino-2-phenylindole (DAPI). As indicated for the rows, the H3-3mK27 antibody was incubated with an H3-3mK27 and an H3-3mK9 peptide, respectively, before the immunostaining was performed.



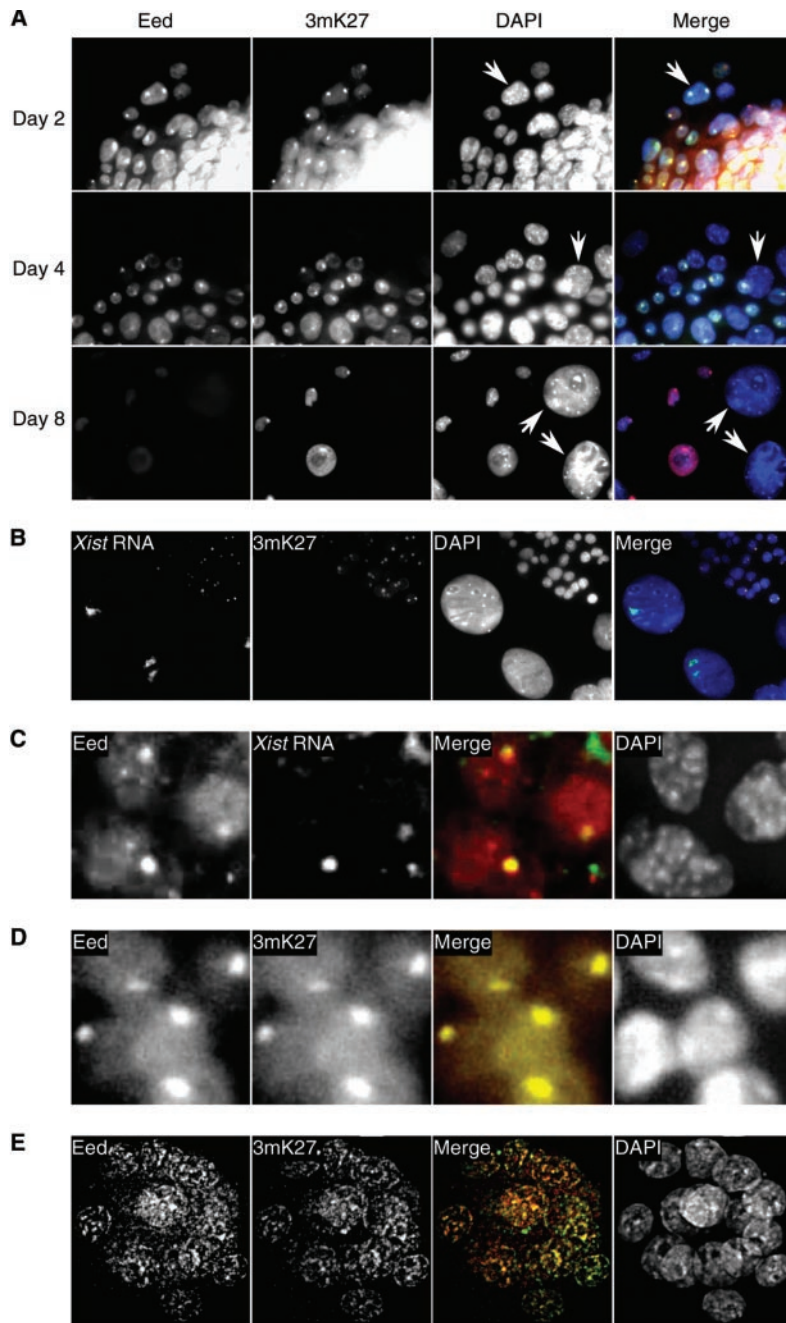


Fig. 2. Enrichment of the Eed-Ezh2 complex and H3-3mK27 on the Xi is transient in extraembryonic cells. **(A)** Immunostaining for Eed and H3-3mK27 in DAPI-stained nuclei of blastocysts cultured for 2, 4, and 8 days. Each row shows a field of cells at the periphery of the blastocyst for one time point. Peripheral fields were chosen because giant cells (some are indicated by arrows) are most easily visualized at the periphery of cultured blasts. The merged images of nuclei (blue), Eed (green), and H3-3mK27 (red) show that at the latest time point, Eed and H3-3mK27 were no longer detectably enriched on the Xi in the large giant cells. **(B)** *Xist* RNA coats the Xi even when there is no detectable Xi enrichment of H3-3mK27 in giant cells. Detection of *Xist* RNA and H3-3mK27 in cells at the periphery of a blastocyst that was cultured for 8 days. The merged image shows the overlap of *Xist* RNA (green) and H3-3mK27 (red) in a subset of nuclei (blue). **(C)** Detection of Eed and *Xist* RNA in trophoblast cells of a blastocyst. The merged image shows colocalization of Eed (red) and *Xist* RNA (green) on the Xi. **(D)** Trophoblast cells of a blastocyst stained with Eed and H3-3mK27 antibodies. The merged image consisting of Eed (red) and H3-3mK27 (green) shows that H3-3mK27 colocalizes with Eed in an Xi-like pattern. **(E)** Eed and H3-3mK27 are not enriched on the X chromosome when X inactivation has not yet occurred. A morula stained with Eed and H3-3mK27 antibodies and DAPI. Deconvolution microscopy was used to demonstrate the nuclear pattern of Eed and H3-3mK27. The merged image demonstrates that there is no obvious focal accumulation of Eed (red) or H3-3mK27 (green) in the cells of this morula. All morula analyzed showed this distribution.

(12), we examined whether the Eed-Ezh2 complex and H3-3mK27 are enriched on the Xi in trophoblast giant cells. Giant cells are differentiated trophoblast cells that are easily identified in cultured blastocysts because of their large size. To allow differentiation of trophoblast giant cells, blastocysts were plated for 2, 4, and 8 days, and the distribution of Eed and H3-3mK27 was determined. We observed an unexpected progressive loss of the Eed and H3-3mK27 staining on the Xi in giant cells (Fig. 2A). Two days after plating, the giant cells of female blastocysts showed a strong Xi staining pattern of Eed and H3-3mK27. After 4 days in culture, the Xi staining of Eed and H3-3mK27 was considerably weaker, and many giant cells lacked any detectable staining. By day 8 in culture, most of the giant cells showed no nuclear staining with antibodies against Eed or H3-3mK27. Immunostaining for H3-3mK27 combined with fluorescence in situ hybridization (FISH) for *Xist* RNA in giant cells on day 8 after plating demonstrated that *Xist* RNA continues to coat the Xi, despite the absence of a detectable enrichment of H3-3mK27 (Fig. 2B). Similar data were obtained with differentiating TS cells (fig. S3). These results show that there is no enrichment of the Eed-Ezh2 complex and H3-3mK27 on the Xi during the maintenance stage of X inactivation in differentiated trophoblast cells, which suggests that the Eed-Ezh2 complex functions during the earlier, initiation stage of X inactivation. Indeed, our data indicate that recruitment of the Eed-Ezh2 complex coincides with the initiation of X inactivation in trophoblast cells. X inactivation occurs in trophoblast cells concomitant with their formation at the blastocyst stage. Trophoblast cells of female blastocysts showed an Xi enrichment for Eed and H3-3mK27 (Fig. 2, C and D), whereas cells of morulae, the developmental stage that precedes the blastocyst stage and in which X inactivation has not yet occurred, did not exhibit localized enrichment of the Eed-Ezh2 complex and K27 methylation (Fig. 2E).

X-chromosome inactivation defects were reported in extraembryonic cells, but not embryonic cells, of *eed* mutant embryos (12). Therefore, it was unexpected to find that the Eed-Ezh2 complex and H3-3mK27 are also enriched on the Xi during the initiation of X inactivation in embryonic cells. To this end, we analyzed the distribution of the Eed-Ezh2 complex and H3-3mK27 in the inner cell mass (ICM) of blastocysts. The ICM will give rise to extraembryonic and embryonic cells, and X inactivation occurs when the cells of the ICM differentiate. We observed that the cells of the ICM of female blastocysts showed abundant, uniform nuclear Eed and

H3-3mK27 staining (15), consistent with the lack of X inactivation in these cells at this stage. In blastocysts plated for 4 days, many ICM-derived cells with obvious embryonic cell morphology have differentiated and showed an Xi-like pattern of Eed and H3-3mK27 accumulation (Fig. 3A, fig. S4). We next used ES cells to study the transient nature of the Xi enrichment of the Eed-Ezh2 complex in embryonic cells. ES cells are derived from the ICM and they initiate X inactivation when they are induced to differentiate. Immunostaining for Ezh2 and H3-3mK27, respectively, demonstrated that Ezh2 and H3-3mK27 are distributed uniformly throughout the nucleus in undifferentiated ES cells (16), consistent with the fact that X inactivation has not yet occurred. X inactivation was initiated shortly after ES cells were induced to differentiate, as marked by the appearance of an *Xist* RNA-coated Xi (Fig. 3B). At this point, the *Xist* RNA-coated Xi was almost always coincident with a region of Ezh2 and H3-3mK27 enrichment, respectively (Fig. 3B). Over time, the proportion of cells that showed an accumulation of Ezh2 and H3-3mK27 on the Xi decreased, until all cells showed a uniform nuclear staining of Eed-Ezh2 complex components, and most cells no longer exhibited accumulation of H3-3mK27 on the Xi (Fig. 3B). Taken together, our data indicate that both embryonic and extraembryonic cell types are characterized by a transient enrichment of the Eed-Ezh2-complex and H3-3mK27 on the Xi during initiation of X inactivation. The transient nature of the enrichment of both the PcG complex and H3-K27 methylation in very different cell types supports the conclusion that the Eed-Ezh2 complex mediates this histone modification on the Xi. It is important to note, however, that H3-3mK27 enrichment on the Xi can persist in some differentiated ES cells and in some somatic cells, at times when the Eed-Ezh2 complex is no longer enriched on the Xi (17).

As ES cells and cells of the ICM can differentiate into both embryonic and extraembryonic cell types, and because only the later cell types showed X inactivation defects in *eed* mutant mice, it remained possible that only cells differentiating down the extraembryonic lineage would show a transient recruitment of the Eed-Ezh2 complex. To determine unequivocally whether cells derived from the embryonic lineage could show enrichment of the EED-EZH2 complex and whether *XIST* RNA can recruit components of this complex, we introduced a tetracycline-inducible promoter-driven human *XIST* cDNA transgene into HeLa cells, which are of the embryonic lineage. Although HeLa is a female cell line, these cells do not contain an *XIST*

RNA-coated Xi (fig. S5A). Two days after expression of the *XIST* transgene was induced, cells that showed a pattern of *XIST* RNA distribution consistent with chromosome coating also exhibited enrichment of EED (Fig. 4A), and H3-3mK27 staining coincided with the region of EED enrichment in these cells (fig. S5B). After prolonged expression of the *XIST* RNA from a cDNA transgene driven by a constitutive cytomegalovirus (CMV) promoter, we did not detect any enrichment of EED in regions of the *XIST* RNA accumulation (Fig. 4, B and C). Thus, *XIST* expression is sufficient for transient recruitment of the EED-EZH2 complex and the H3-K27 methylation on the Xi in cells of the embryonic lineage. Furthermore, these data indicate that the *XIST* RNA-mediated recruitment of the complex and concomitant H3-K27 methylation are not limited to a developmental window.

To test whether X-chromosome silencing is necessary for recruitment of the Eed-Ezh2 complex to the Xi, we used a male ES cell line carrying an inducible mutant *Xist* cDNA transgene. When induced, this cell line (T20:ΔSX) produces a mutant *Xist* RNA that coats the X chromosome but does not silence it (18). Ezh2 and H3-K27 methylation are enriched on the *Xist* RNA-coated, active X chromosome when *Xist* expression is induced in these cells (Fig. 4, D and E). These results indicate that recruitment of the Eed-Ezh2 complex to the Xi does not depend on the silencing function of *Xist* RNA and that the recruitment of the Eed-Ezh2 complex and the H3-3mK27 mark are not suf-

ficient for X-chromosome silencing. Using this cell line, we also demonstrated that coating by *Xist* RNA is continually required for the recruitment of the Eed-Ezh2 complex and H3-3mK27 on the X chromosome in undifferentiated ES cells, because this enrichment is no longer detected when the *Xist* cDNA transgene is silenced (16).

Our data suggest that the initial coating of the chromosome by *Xist* RNA results in transient recruitment of the Eed-Ezh2 complex, which in turn trimethylates H3 at Lys²⁷. Coating of the chromosome by *Xist* RNA is sufficient, as well as necessary, for enrichment of the Eed-Ezh2 complex and the accompanying H3-3mK27 methylation. The developmental timing of Eed-Ezh2 complex recruitment to the Xi strongly suggests a role for this PcG complex in initiation of X inactivation in both embryonic and extraembryonic lineages. However, *eed* mutant embryos are competent for initiation of X inactivation in all cell types and fail to maintain the Xi only in extraembryonic cells (12). It is important to note that it is unclear whether embryonic cells in *eed* mutant embryos showed defects in X inactivation. The assay for X-chromosome silencing in the *eed* mutant background involved reactivation of a paternal X-linked green fluorescent protein (GFP) transgene (12). In extraembryonic cells, in which X inactivation is imprinted such that the paternally inherited X chromosome is always silenced, the GFP transgene provides an accurate reflection of defects in X inactivation. However, in embryonic cells, where X inactivation occurs at random, only

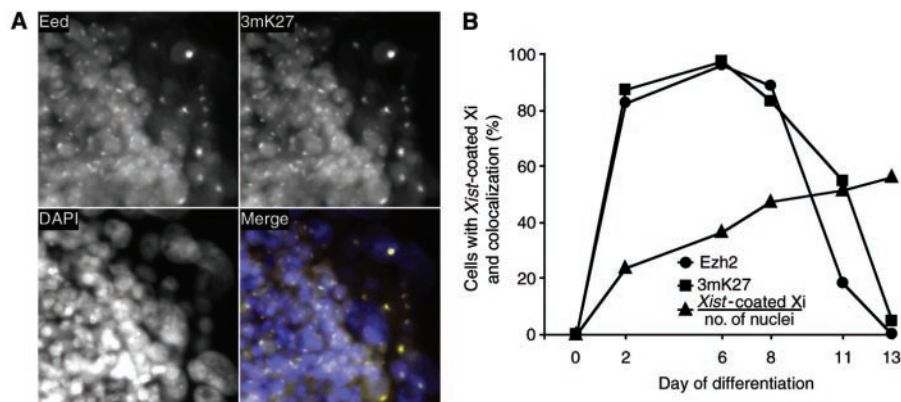


Fig. 3. The Eed-Ezh2 complex and the H3-3mK27 mark are transiently recruited to the Xi in embryonic cells. (A) Eed and H3-3mK27 show an Xi-like enrichment in the ICM region of cultured female blastocysts. Blastocysts were cultured for 4 days, to allow differentiation of ICM cells, and stained for Eed and H3-3mK27. The merged image shows colocalization of Eed (green) and H3-3mK27 (red) in an Xi-like pattern in nuclei of ICM cells (blue). Because the ICM is a structure of many cell layers, it is impossible to show a focal plane that shows Xi-like staining in all cells. However, focusing through the ICM suggested that the majority of cells showed an Xi-like pattern of Eed and H3-3mK27 accumulation. (B) Transient enrichment of the Eed-Ezh2 complex during initiation of X inactivation in differentiating female mouse ES cells. The graph shows the percentage of cells with *Xist* RNA coating of the Xi (triangles), and the proportion of these cells that show colocalization with Ezh2 (circles) and H3-3mK27 (squares) at different time points during differentiation of female ES cells ($n > 100$ for each). Transient enrichment of the Eed/Ezh2 complex on the Xi was observed in all time courses ($n = 10$; not shown).

REPORTS

half the cells would be expected to show silencing of the GFP transgene. As reactivation of the Xi occurred in only a fraction of extraembryonic cells in *eed* mutant mice (12), reactivation in a minor proportion of embryonic cells would have been extremely

difficult to detect and cannot be excluded. Our data indicate that the Eed-Ezh2 complex regulates X inactivation in extraembryonic and embryonic cell types.

Recruitment of the Eed-Ezh2 complex occurs transiently during initiation of X

inactivation, and Eed is required during maintenance. To resolve this seeming contradiction, we suggest that the Xi enrichment of H3-3mK27 mediated by the Eed-Ezh2 complex during initiation, directly or indirectly, recruits an additional activity that is required for maintenance of X-chromosome silencing. Although the Polycomb protein, a component of the PcG complex PRC1, binds to methylated H3-K27 in vitro (8–10) and is required to maintain PcG silencing (19), no enrichment of PcG proteins on the Xi in somatic cells has been reported, which suggests that the mammalian PRC1 complex may not be involved in maintenance of X-chromosome silencing.

Alternatively, it is possible that a function of *eed* during initiation of X inactivation was masked in *eed* mutant mice by maternal stores of the wild-type mRNA and protein. X inactivation is initiated in the majority of cells before embryonic day 5.5 (12), when wild-type embryos appear to rely largely on maternally derived Eed (20). In *eed* mutant mice, maternally supplied Eed should be present, and X inactivation should initiate normally, at least in some cells. To explain the patchy reactivation of the Xi in a small number of *eed* mutant extraembryonic cells, we suggest that there is a window in which X inactivation is dependent on continued recruitment of Eed to the Xi by *Xist* RNA. There is a precedent for such a window. X inactivation is dependent on continued *Xist* expression for the first 2 days after *Xist* RNA coats the chromosome after ES cells differentiate (21). Eed is enriched on the Xi in this *Xist*-dependent initiation phase of X inactivation. Reactivation of the Xi in a subset of *eed* mutant cells could result from depletion of maternal stores in these cells while they are still in the *Xist*- and Eed-dependent phase of X inactivation. We speculate that the role of the Eed-Ezh2 complex and the accompanying H3-K27 methylation in initiation of X inactivation may be to facilitate the initial rounds of chromosome coating by *Xist* RNA or to regulate the activity of additional proteins that are recruited to mediate silencing.

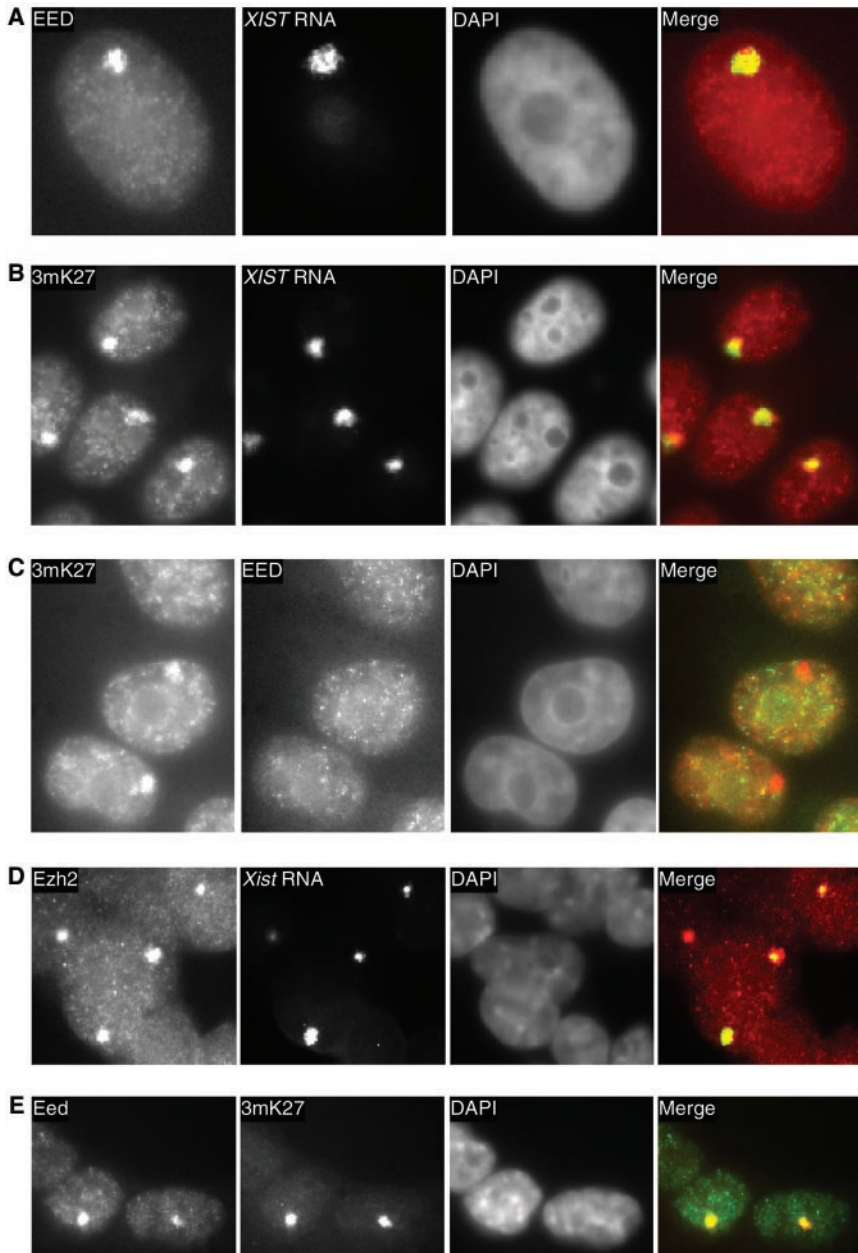


Fig. 4. *XIST/Xist* RNA is sufficient to recruit the PcG complex and the H3-K27 mark, and the silencing function of the RNA is not required for this recruitment. DAPI marks the nuclei of cells in all panels. (A) HeLa cells, in which expression of *XIST* from a cDNA transgene was induced for 2 days, were stained for EED and *XIST* RNA. The merged image shows colocalization of EED (red) and the *XIST* RNA (green). (B and C) HeLa cells that were expressing *XIST* RNA from a constitutive promoter for several weeks were analyzed for distribution of (B) H3-3mK27 (red in merge) and *XIST* RNA (green in merge) and (C) H3-3mK27 (red in merge) and EED (green in merge). After prolonged *XIST* expression, EED is not enriched on the *XIST*-coated Xi, indicating that the recruitment of the EED-EZH2 complex is transient when *XIST* is ectopically expressed in HeLa cells. The H3-3mK27 methylation persists although EED is no longer enriched on the Xi, as was observed with some other cell types (22). (D and E) DAPI marks the nuclei of cells in both panels. Mouse ES cells induced to express a mutant form of *Xist* RNA that can coat but not silence the chromosome were analyzed for distribution of (D) *Xist* RNA (green in merge) and Ezh2 (red in merge) and (E) H3-3mK27 (red) and Eed (green).

References and Notes

1. P. Avner, E. Heard, *Nature Rev. Genet.* **2**, 59 (2001).
2. K. Plath, S. Mlynarczyk-Evans, D. A. Nusinow, B. Panning, *Annu. Rev. Genet.* **36**, 233 (2002).
3. R. M. Boumil, J. T. Lee, *Hum. Mol. Genet.* **10**, 2225 (2001).
4. N. Brockdorff, *Trends Genet.* **18**, 352 (2002).
5. Y. Zhang, D. Reinberg, *Genes Dev.* **15**, 2343 (2001).
6. T. Kouzarides, *Curr. Opin. Genet. Dev.* **12**, 198 (2002).
7. T. Jenuwein, C. D. Allis, *Science* **293**, 1074 (2001).
8. R. Cao et al., *Science* **298**, 1039 (2002).
9. B. Czermin et al., *Cell* **111**, 185 (2002).
10. A. Kuzmichev, K. Nishioka, H. Erdjument-Bromage, P. Tempst, D. Reinberg, *Genes Dev.* **16**, 2893 (2002).
11. J. Muller et al., *Cell* **111**, 197 (2002).
12. J. Wang et al., *Nature Genet.* **28**, 371 (2001).
13. W. Mak et al., *Curr. Biol.* **12**, 1016 (2002).
14. R. Cao and Y. Zhang, unpublished results.
15. K. A. Worringer and B. Panning, unpublished data.
16. K. Plath and B. Panning, unpublished results.
17. _____, unpublished results.

18. A. Wutz, T. P. Rasmussen, R. Jaenisch, *Nature Genet.* **30**, 167 (2002).
 19. J. A. Simon, J. W. Tamkun, *Curr. Opin. Genet. Dev.* **12**, 210 (2002).
 20. A. Schumacher, C. Faust, T. Magnuson, *Nature* **384**, 648 (1996).
 21. A. Wutz, R. Jaenisch, *Mol. Cell* **5**, 695 (2000).
 22. B. Panning, unpublished data.
 23. We thank G. Uy, R. Jaenisch, and T. Magnuson for reagents; V. Nguyen and D. Scheel for preimplan-

tation embryos; A. Andersen, D. Nusinow, and H. Cohen for critical reading of the manuscript. Y.Z. is a Kimmel Scholar and is supported by grants from NIH and the American Chemical Society. B.P. is a Pew Scholar and is funded by NIH and by grants from Howard Hughes Medical Institute and the Sandler Family Foundation. K.P. is an O'Donnell Foundation Fellow of the Life Sciences Research Foundation. S.M.-E. and C.C.C. are supported by a National Sciences Foundation graduate fellowship.

Supporting Online Material

www.sciencemag.org/cgi/content/full/1084274/DC1
 Materials and Methods
 Figs. S1 to S5
 References

24 February 2003; accepted 7 March 2003
 Published online 20 March 2003;
 10.1126/science.1084274
 Include this information when citing this paper.

BAX and BAK Regulation of Endoplasmic Reticulum Ca^{2+} : A Control Point for Apoptosis

Luca Scorrano,^{1,2*} Scott A. Oakes,^{1*} Joseph T. Opferman,¹
 Emily H. Cheng,¹ Mia D. Sorcinelli,¹ Tullio Pozzan,^{2,3}
 Stanley J. Korsmeyer^{1†}

BAX and BAK are "multidomain" proapoptotic proteins that initiate mitochondrial dysfunction but also localize to the endoplasmic reticulum (ER). Mouse embryonic fibroblasts deficient for BAX and BAK (DKO cells) were found to have a reduced resting concentration of calcium in the ER ($[\text{Ca}^{2+}]_{\text{er}}$) that results in decreased uptake of Ca^{2+} by mitochondria after Ca^{2+} release from the ER. Expression of SERCA (sarcoplasmic-endoplasmic reticulum Ca^{2+} adenosine triphosphatase) corrected $[\text{Ca}^{2+}]_{\text{er}}$ and mitochondrial Ca^{2+} uptake in DKO cells, restoring apoptotic death in response to agents that release Ca^{2+} from intracellular stores (such as arachidonic acid, C_2 -ceramide, and oxidative stress). In contrast, targeting of BAX to mitochondria selectively restored apoptosis to "BH3-only" signals. A third set of stimuli, including many intrinsic signals, required both ER-released Ca^{2+} and the presence of mitochondrial BAX or BAK to fully restore apoptosis. Thus, BAX and BAK operate in both the ER and mitochondria as an essential gateway for selected apoptotic signals.

Intracellular organelles are key participants in apoptosis (1). Mitochondria are the best documented of these, but the ER—where members of the BCL-2 family of proteins also localize—has been implicated (2). The proapoptotic BCL-2 family members can be subdivided into "multidomain" and "BH3-only" classes (3). The multidomain proapoptotic members BAX and BAK are necessary for apoptosis in response to a diverse array of intrinsic death signals and extrinsic death receptor signals in type II cells, which require a mitochondrial amplification loop (4). BH3-only proteins reside upstream in the pathway and either directly or indirectly activate BAX and BAK, inducing their intramembranous homooligomerization, which in turn results in the permeabilization of the outer mitochondrial membrane (5, 6). Released intermembrane-

space proteins include cytochrome c, which complexes with Apaf-1 and caspase-9 to form a postmitochondrial apoptosome that amplifies effector caspase activation (7).

The mitochondria and ER are interconnected both physically and physiologically, affecting mitochondrial metabolism and complex cellular processes (8, 9). Mitochondria, the main source of cellular adenosine triphosphate, also modulate and synchronize Ca^{2+} signaling. Stimuli that generate inositol 1,4,5-trisphosphate (IP_3) cause release of Ca^{2+} from the ER, which is rapidly taken up by closely juxtaposed mitochondria (10). Ca^{2+} has long been recognized as a participant in apoptotic pathways (11). Ca^{2+} is also a prominent modulator of mitochondrial permeability transition (PT) controlled by the PT pore (PTP) (12). The PT has been implicated as a mechanism of both apoptotic and necrotic cell death after selected stimuli (2, 13). Overexpression of BCL-2 protects cells from death induced by thapsigargin, an irreversible inhibitor of the SERCA pump responsible for uptake of Ca^{2+} from the cytosol into the ER lumen (14). Cells overexpressing BCL-2 display reduced ER Ca^{2+} concentration and decreased capacitative Ca^{2+} entry (15, 16). Here, we pursued a loss-of-function approach

to assess whether BAX and BAK influence Ca^{2+} dynamics.

Thapsigargin causes the passive release of Ca^{2+} from ER stores and an increase in cytosolic Ca^{2+} ($[\text{Ca}^{2+}]_i$) that we measured with the dye Fura-2. The increase in $[\text{Ca}^{2+}]_i$ in DKO cells [mouse embryo fibroblasts (MEFs) deficient for BAX and BAK] was smaller than that in wild-type cells (Fig. 1A). Primary as well as SV40-immortalized DKO MEFs displayed identical defects. Consequently, the multiply repeated assays in this study were performed on cell lines after confirmation of the same effect in primary cells. Moreover, MEFs singly deficient for BAX or BAK displayed similar but intermediate amounts of Ca^{2+} release, suggesting a comparable influence of each gene. The transient increase in $[\text{Ca}^{2+}]_i$ elicited by thapsigargin in cells exposed to no extracellular Ca^{2+} was also significantly reduced in DKO cells relative to wild-type cells (Fig. 1B). The extent of capacitative Ca^{2+} entry assessed by addition of extracellular Ca^{2+} was similar in wild-type and DKO cells (Fig. 1B). Histamine caused IP_3 -mediated release of Ca^{2+} from ER pools and resulted in a significantly lower peak $[\text{Ca}^{2+}]_i$ in DKO cells (Fig. 1C). Thus, the rise in $[\text{Ca}^{2+}]_i$ elicited by discharge of intracellular Ca^{2+} stores is diminished in cells that lack BAX and BAK.

The lipid mediators C_2 -ceramide and arachidonic acid (ArA) are proposed to initiate apoptotic death by a Ca^{2+} -controlled process that induces the mitochondrial PT and can be inhibited by cyclosporin A (CsA) (17–19). These second messengers participate in death pathways initiated by cell surface receptors, DNA damage, and chemotherapy. C_2 -ceramide (40 μM) (Fig. 1D) and ArA (60 μM) (Fig. 1E) caused release of Ca^{2+} in wild-type cells, which was markedly blunted in DKO cells. Ca^{2+} release was also observed in the absence of extracellular Ca^{2+} , which suggests that these stimuli mobilized intracellular stores. We used H_2O_2 as a representative oxidant; at 1 mM, H_2O_2 induces cell death that has apoptotic morphology, requires BAX or BAK, and can be inhibited by overexpressed BCL-2 (20). Again, the DKO cells proved defective in mobilization of Ca^{2+} (Fig. 1F).

Immunolocalization studies have suggested that endogenous BAX and BAK localize to the ER as well as to mitochondria (21, 22). We used a combination of immunoelectron microscopy, confocal imaging, and subcellu-

¹Howard Hughes Medical Institute, Dana-Farber Cancer Institute, Brigham and Women's Hospital, Department of Pathology and Medicine, Harvard Medical School, Boston, MA 02115, USA. ²Venetian Institute for Molecular Medicine, 35121 Padova, Italy. ³Department of Biomedical Sciences, University of Padova, 35121 Padova, Italy.

*These authors contributed equally to this work.

†To whom correspondence should be addressed. E-mail: stanley_korsmeyer@dfci.harvard.edu